

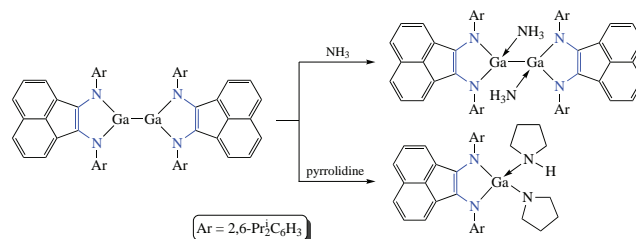
## Reactivity of digallane toward nitrogen-containing compounds

Tatyana S. Koptseva, Natalia L. Bazyakina, Evgeny V. Baranov and Igor L. Fedushkin\*

 G. A. Razuvaev Institute of Organometallic Chemistry, Russian Academy of Sciences,  
603137 Nizhny Novgorod, Russian Federation. E-mail: igorfed@iomc.ras.ru

DOI: 10.1016/j.mencom.2023.02.006

The reactions of [LGa–GaL] (L = dpp-bian = 1,2-bis[(2,6-diisopropylphenyl)imino]acenaphthene) with ammonia and pyrrolidine in toluene lead to the formation of adducts [L(NH<sub>3</sub>)Ga–Ga(NH<sub>3</sub>)L], [L(HNC<sub>4</sub>H<sub>8</sub>)Ga–GaL] and [L(HNC<sub>4</sub>H<sub>8</sub>)Ga–Ga(HNC<sub>4</sub>H<sub>8</sub>)L], respectively. In contrast, the reaction between crystalline digallane and an excess of pyrrolidine leads to the formation of compound [LGa(NC<sub>4</sub>H<sub>8</sub>)(HNC<sub>4</sub>H<sub>8</sub>)]. The complex [LGa(C<sub>5</sub>H<sub>5</sub>N)(μ-O)Ga(C<sub>5</sub>H<sub>5</sub>N)L] was obtained from reaction of digallane with N<sub>2</sub>O in the presence of pyridine.



**Keywords:** gallium compounds, redox-active ligands, nitrogen compounds, small molecules, X-ray diffraction.

*Dedicated to Professor Irina P. Beletskaya on occasion of her anniversary.*

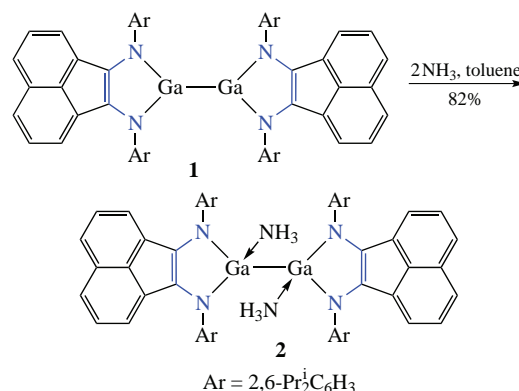
The activation of organic and small molecules for their further chemical transformation has been a point of interest in organometallic chemistry for decades. Although transition metal compounds still dominate in the chemistry of activation and modification of various substrates, the use of non-transition element complexes in this field is increasing significantly. In particular, the usage of low-valent as well as metal–metal bonded species of the p-block elements represents a successful approach to the transformation of many organic and inorganic derivatives.<sup>1–4</sup> Thus, the reactivity of Ga<sup>I</sup> and Al<sup>I</sup> compounds displays examples of oxidative addition of E–H (E = H, C, N, B, Si),<sup>1,5–11</sup> C–X (X = F, Cl, O, S)<sup>12–15</sup> bonds and activation of multiple bonds.<sup>5,6,16</sup> Some derivatives with a M–M bond (M = Al, Ga) are also capable of cleaving double bonds<sup>4,17–21</sup> and reacting in two-electron oxidative addition manner.<sup>17,22,23</sup> This often becomes possible due to the presence of the double M=M bond or the redox-active ligand in them. In particular, the redox-active diimine ligands are capable of reversibly accepting and releasing electrons, as well as directly participating in the formation and cleavage of chemical bonds with substrates. Metal–ligand cooperativity in the complexes helps them to mobilize either electrons of the metal–metal bond, or of the ligand, or of both. This is appeared in a unique reactivity of compounds which contain this type of ligands.<sup>4</sup>

Previously, we have demonstrated that complex (dpp-bian)Ga–Ga(dpp-bian) **1** (dpp-bian is dianion of 1,2-bis[(2,6-diisopropylphenyl)imino]acenaphthene), in addition to the cycloaddition reactions of alkynes, isocyanates and isothiocyanates<sup>4</sup> and two-electron oxidative addition of organic halides,<sup>23</sup> could catalyze hydroamination of alkynes and carbodiimides.<sup>24,25</sup> This makes it interesting to understand the chemical behaviour of digallane toward nitrogen-containing compounds. Here, we report on the reactivity of digallane toward ammonia, pyrrolidine and N<sub>2</sub>O.

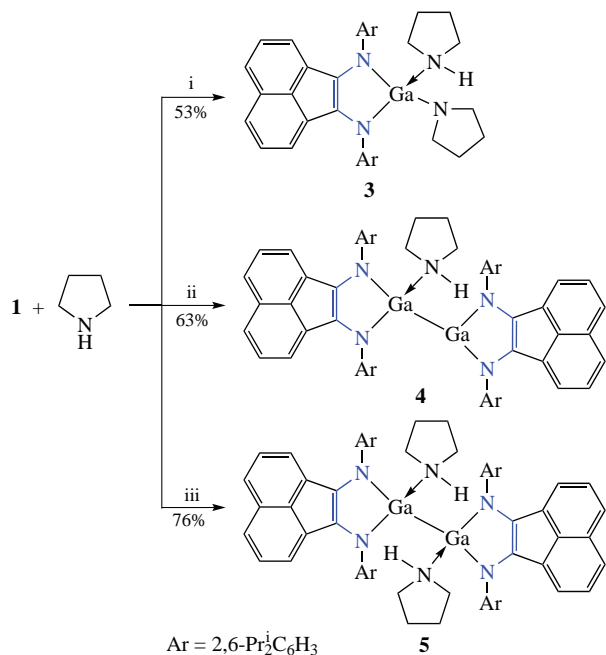
The addition of an excess of NH<sub>3</sub> to a frozen solution of **1** in toluene causes the change in the colour of the reaction

mixture from deep blue to green and the formation of adduct [(dpp-bian)(NH<sub>3</sub>)Ga–Ga(NH<sub>3</sub>)(dpp-bian)] **2** as green crystals (82%, Scheme 1). Warming of the reaction flask to approximately 50 °C resulted in restoration of the initial deep-blue colour of digallane **1**. In the IR spectrum of **2**, the N–H vibrations appear as intense bands at 3272 and 3360, 3375 cm<sup>–1</sup>. The <sup>1</sup>H NMR spectrum in THF-*d*<sub>8</sub> (Figures S3) contains the expected set of signals of dpp-bian and ammonia ligands.

Example of oxidative addition of an ammonia molecule to Ga<sup>I</sup> derivatives is known.<sup>10</sup> However, in the case of complex **1**, the reaction stops at the stage of coordination of the NH<sub>3</sub> molecule by the gallium atom, even when the reaction is carried out in liquid ammonia. Meanwhile, the addition of an excess of pyrrolidine to crystalline digallane leads to compound **3** of another type, [(dpp-bian)Ga(NC<sub>4</sub>H<sub>8</sub>)(HNC<sub>4</sub>H<sub>8</sub>)] (53%, Scheme 2). Blue crystals of **3** suitable for X-ray diffraction were obtained from toluene–hexane mixture. Compound **3** is apparently generated from unstable intermediate [(dpp-bian)Ga(H)(NC<sub>4</sub>H<sub>8</sub>)] through the reductive elimination of



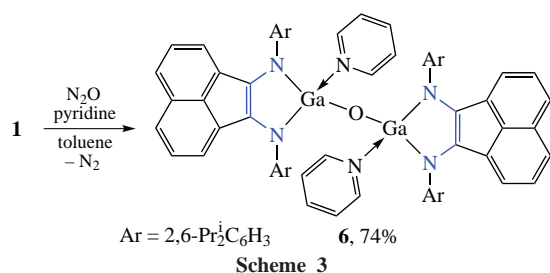
Scheme 1



**Scheme 2** Reagents and conditions: i, pyrrolidine (excess), 50 °C; ii, pyrrolidine (1 equiv.), toluene, 25 °C, 24 h; iii, pyrrolidine (36 equiv.), toluene, 25 °C, 24 h.

hydrogen. Previously,<sup>26,27</sup> we observed similar processes during the study of acenaphthene-1,2-diimine hydrides of aluminum and gallium. In its turn, the addition of one equivalent or an excess of pyrrolidine to a solution of digallane **1** in toluene affords adducts [(dpp-bian)(HNC<sub>4</sub>H<sub>8</sub>)Ga–Ga(dpp-bian)] **4** (63%) or [(dpp-bian)(HNC<sub>4</sub>H<sub>8</sub>)Ga–Ga(HNC<sub>4</sub>H<sub>8</sub>)(dpp-bian)] **5** (76%), respectively (see Scheme 2). Complex **4** was isolated as brown crystals, whereas compound **5** as green crystals. In the IR spectra of **3–5**, the N–H vibrations appear as intense bands at 3275, 3292 and 3278 cm<sup>-1</sup>, respectively. The <sup>1</sup>H NMR spectra of compounds **3–5** (Figures S4, S6, S7) contain the signals of coordinated dpp-bian and pyrrolidine ligands.

We have demonstrated that oxidation of digallane **1** with N<sub>2</sub>O in toluene resulted in a paramagnetic oxo-bridged compound [(dpp-bian)Ga(μ<sub>2</sub>-O)<sub>2</sub>Ga(dpp-bian)].<sup>28</sup> Similarly, the β-diketiminato complex [NaCnacGa] reacts with N<sub>2</sub>O to give compound [NaCnacGa(μ-O)]<sub>2</sub>.<sup>29</sup> However, Nikonov *et al.*<sup>11</sup> demonstrated recently that reaction between [NaCnacGa] and nitrous oxide in the presence of pyridine led to the product of C–H activation of pyridine [NaCnacGa(OH)(*o*-C<sub>5</sub>H<sub>4</sub>N)]. In our experiments, the reaction of digallane **1** with N<sub>2</sub>O and pyridine proceeded towards the formation of a dianionic oxo-bridged complex [(dpp-bian)Ga(C<sub>5</sub>H<sub>5</sub>N)(μ-O)Ga(C<sub>5</sub>H<sub>5</sub>N)(dpp-bian)] (**6**, 74%). In the first step of the reaction, apparently, the coordination of pyridine by gallium atoms takes place, and in the second step, the adduct [(dpp-bian)Ga(C<sub>5</sub>H<sub>5</sub>N)–Ga(C<sub>5</sub>H<sub>5</sub>N)(dpp-bian)] is oxidized with N<sub>2</sub>O. Thus, due to the presence of a strong Lewis base on the metal atom, the acenaphthenediimine ligand saves the dianionic state.<sup>27</sup> Compound **6** was isolated as green crystals.



New complexes **2–6** have been characterized by the single crystal X-ray analysis<sup>†</sup> (Figures 1–3, S1, S2 and Tables S1, S2, see Online Supplementary Materials). In all complexes interatomic distances of diimine moieties are close to those in the original digallane [N(1)–C(1) 1.393(3) Å; N(2)–C(2) 1.389(3) Å; C(1)–C(2) 1.375(3) Å] (Table S1), which confirms dianionic character of dpp-bian ligands.<sup>30</sup> Compounds **2**, **5** and **6** represent dinuclear four-coordinate gallium complexes. In complex **2** both gallium atoms coordinate ammonia, in complex

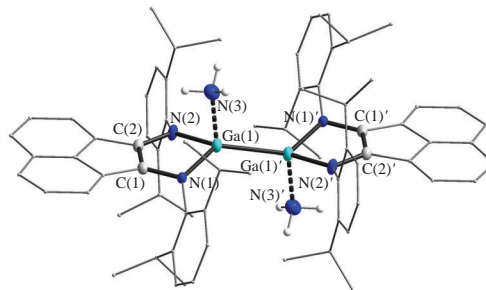


**Figure 1** Molecular structure of compound **2**. Thermal ellipsoids drawn at 50% probability level.

<sup>†</sup> Crystal data for **2**. C<sub>72</sub>H<sub>86</sub>Ga<sub>2</sub>N<sub>6</sub>, *M* = 174.90, 100(2) K, monoclinic, space group *P*2<sub>1</sub>/*n*, *a* = 13.7390(7), *b* = 13.9627(7) and *c* = 16.0243(8) Å,  $\alpha = 90^\circ$ ,  $\beta = 99.337(2)^\circ$ ,  $\gamma = 90^\circ$ , *V* = 3033.3(3) Å<sup>3</sup>, *Z* = 2, *d*<sub>calc</sub> = 1.286 Mg m<sup>-3</sup>.

Crystal data for **3**. C<sub>44</sub>H<sub>57</sub>Ga<sub>2</sub>N<sub>4</sub>, *M* = 711.65, 100(2) K, monoclinic, space group *P*2<sub>1</sub>/*c*, *a* = 10.5539(9), *b* = 20.4624(13) and *c* = 17.8849(13) Å,  $\alpha = 90^\circ$ ,  $\beta = 102.900(8)^\circ$ ,  $\gamma = 90^\circ$ , *V* = 3764.9(5) Å<sup>3</sup>, *Z* = 4, *d*<sub>calc</sub> = 1.256 Mg m<sup>-3</sup>.

Crystal data for **4**. C<sub>85.5</sub>H<sub>107</sub>Ga<sub>2</sub>N<sub>5</sub>, *M* = 1344.19, 100(2) K, triclinic, space group *P*1̄, *a* = 12.0662(16), *b* = 13.0749(17) and *c* = 26.069(4) Å,  $\alpha = 104.388(2)^\circ$ ,  $\beta = 91.883(3)^\circ$ ,  $\gamma = 113.391(2)^\circ$ , *V* = 3616.2(9) Å<sup>3</sup>, *Z* = 2, *d*<sub>calc</sub> = 1.234 Mg m<sup>-3</sup>.

Crystal data for **5**. C<sub>80</sub>H<sub>98</sub>Ga<sub>2</sub>N<sub>6</sub>, *M* = 1283.08, 100(2) K, orthorhombic, space group *Pnma*, *a* = 27.7611(11), *b* = 21.1364(9) and *c* = 11.5765(5) Å,  $\alpha = \beta = \gamma = 90^\circ$ , *V* = 6792.7(5) Å<sup>3</sup>, *Z* = 4, *d*<sub>calc</sub> = 1.255 Mg m<sup>-3</sup>.

Crystal data for **6**. C<sub>97</sub>H<sub>105</sub>Ga<sub>2</sub>N<sub>6</sub>O, *M* = 1510.30, 100(2) K, monoclinic, space group *P*2<sub>1</sub>/*n*, *a* = 16.2793(8), *b* = 24.1339(12) and *c* = 21.3756(10) Å,  $\alpha = 90^\circ$ ,  $\beta = 101.791(2)^\circ$ ,  $\gamma = 90^\circ$ , *V* = 8220.9(7) Å<sup>3</sup>, *Z* = 4, *d*<sub>calc</sub> = 1.220 Mg m<sup>-3</sup>.

The X-ray diffraction data for **2–6** were collected on a Bruker D8 Quest (for **2**, **4–6**) and Agilent Xcalibur E (for **3**) diffractometers using the APEX3<sup>32</sup> and CrysAlisPro<sup>33</sup> software packages, respectively. The intensity data were integrated by SAINT<sup>34,35</sup> (for **2**, **4–6**) and CrysAlisPro<sup>33</sup> (for **3**) programs. SADABS<sup>36</sup> (for **2**, **4–6**) and SCALEABSPACK<sup>37</sup> (for **3**) were used to perform area-detector scaling and absorption corrections. All structures were solved by direct methods with dual-space algorithm<sup>38</sup> and refined on *F*<sub>hkl</sub><sup>2</sup> using SHELXTL package.<sup>39,40</sup> All non-hydrogen atoms were refined anisotropically. Hydrogen atoms were placed in calculated positions and refined using a riding model [*U*<sub>iso</sub>(H) = 1.5 *U*<sub>eq</sub>(C) for Me-group and *U*<sub>iso</sub>(H) = 1.2 *U*<sub>eq</sub>(C) for other groups]. H atoms of NH<sub>3</sub> groups in **2** and at the nitrogen atom of pyrrolidine ligands in **3–5** were found from the Fourier synthesis of the electron density and refined isotropically. Me-groups of some Pr<sup>i</sup> substituents in dpp-ligands were located to be disordered over two positions. Coordinated pyrrolidine molecules in **5** are disordered over two positions due to a mirror plane of symmetry passing through the digallane complex. Crystal of **4** contains one *n*-hexane and 0.5 toluene molecules per one Ga complex, the solvent molecules are disordered over two sites in common and special positions, respectively. In crystal of **6**, there were found 2.5 benzene molecules per one gallium complex; some of benzene molecules are disordered over two sites in common and special positions as well.

CCDC 2209489 (**2**), 2209490 (**3**), 2209491 (**4**), 2209492 (**5**) and 2209493 (**6**) contain the supplementary crystallographic data for this paper. These data can be obtained free of charge from The Cambridge Crystallographic Data Centre via <http://www.ccdc.cam.ac.uk>.

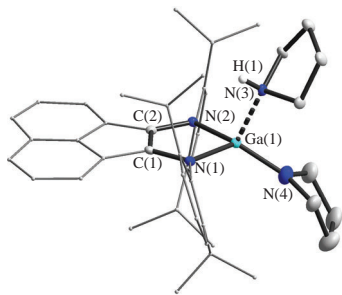


**Figure 2** Molecular structure of compound **3**. Thermal ellipsoids drawn at 20% probability level.

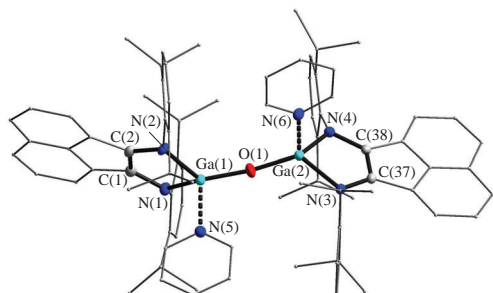


**Figure 3** Molecular structure of compound **6**. Thermal ellipsoids drawn at 50% probability level.

**5** they are bonded with pyrrolidine, and in complex **6** with pyridine. Complex **4** contains three- and four-coordinate gallium atoms, the latter coordinates the pyrrolidine ligand. Due to rise of the coordination number from three to four on going from **1** to **2**, **4** and **5**, the metal–metal bond lengths in **2** [2.4421(7) Å], **4** [2.4167(6) Å] and **5** [2.4695(5) Å] are longer compared to that in **1** [2.3598(3) Å]. Compound **6** contains O<sup>2-</sup> ligand connecting two metal fragments. The Ga–O(1) distances in complex **6** [1.756(2) and 1.757(2) Å] fall in the range of those bond distances in other gallium oxides.<sup>28,29</sup> The interatomic distances Ga–N(5) [2.049(2) Å], Ga–N(6) [2.038(2) Å] in compound **6** are similar to the same bond in the complex [(dpp-bian)Ga(H)(C<sub>5</sub>H<sub>5</sub>N)] [2.0535(12) Å]<sup>27</sup> and shorter than distances Ga–N in the coordination polymer [(dpp-bian)Ga–Zn(dpp-bian)(μ<sup>2</sup>-1,3-Py<sub>2</sub>(CH<sub>2</sub>)<sub>3</sub>)<sub>n</sub>] [2.193(3) Å].<sup>31</sup> Compound **3** is a monomeric four-coordination complex of gallium (see Figure 2). The metal atom exhibits a slightly distorted tetrahedral environment. The Ga(1)–N(4) bond length [1.832(4) Å] is shorter than the Ga(1)–N(3) one [2.059(3) Å].

In summary, we have demonstrated that digallane **1** easily coordinated nitrogen-containing compounds such as ammonia and pyrrolidine to afford the corresponding adducts. However, in the case of ammonia, the reaction stops at the stage of coordination of the NH<sub>3</sub> molecule by the gallium atom, even when the reaction is carried out in liquid ammonia. The addition of an excess of pyrrolidine to crystalline digallane results in cleavage of N–H bond of pyrrolidine. The reaction between **1** and N<sub>2</sub>O in the presence of pyridine leads to dianionic oxo-bridged complex, while in pure toluene paramagnetic compound [(dpp-bian)Ga(μ<sub>2</sub>-O)<sub>2</sub>Ga(dpp-bian)] is obtained. This confirms that gallium derivatives with dianionic diimine ligands can be stabilized by a strong Lewis base.

The synthesis of complexes **2** and **6** was supported by the Ministry of Science and Higher Education of the Russian Federation (grant no. MK-1635.2022.1.3). The synthesis of complexes **3–5** was performed in the framework of the Russian state assignment. The study was performed using equipment of the center for collective use ‘Analytical Center of IOMC RAS’ within the Project ‘Ensuring of development of material and

technical infrastructure of the centers for collective use of scientific equipment’ (identification no. RF-2296.61321X0017, agreement no. 075-15-2021-670).

#### Online Supplementary Materials

Supplementary data associated with this article can be found in the online version at doi: 10.1016/j.mencom.2023.02.006.

#### References

- 1 T. Chu and G. I. Nikonov, *Chem. Rev.*, 2018, **118**, 3608.
- 2 S. Dagorne and R. Wehmschulte, *ChemCatChem*, 2018, **10**, 2509.
- 3 L. Greb, F. Ebner, Y. Ginzburg and L. M. Sigmund, *Eur. J. Inorg. Chem.*, 2020, **32**, 3030.
- 4 R. Zhang, Y. Wang, Y. Zhao, C. Redshaw, I. L. Fedushkin, B. Wu and X.-J. Yang, *Dalton Trans.*, 2021, **50**, 13634.
- 5 Y. Liu, J. Li, X. Ma, Z. Yang and H. W. Roesky, *Coord. Chem. Rev.*, 2018, **374**, 387.
- 6 J. Hicks, P. Vasko, J. M. Goicoechea and S. Aldridge, *Angew. Chem., Int. Ed.*, 2021, **60**, 1702.
- 7 T. Chu, I. Korobkov and G. I. Nikonov, *J. Am. Chem. Soc.*, 2014, **136**, 9195.
- 8 Z. Zhu, X. Wang, Y. Peng, H. Lei, J. C. Fettinger, E. Rivard and P. P. Power, *Angew. Chem., Int. Ed.*, 2009, **48**, 2031.
- 9 A. Seifert, D. Scheid, G. Linti and T. Zessin, *Chem. – Eur. J.*, 2009, **15**, 12114.
- 10 C. Jones, D. P. Mills and R. P. Rose, *J. Organomet. Chem.*, 2006, **691**, 3060.
- 11 A. Kassymbek, S. F. Vyboishchikov, B. M. Gabidullin, D. Spasyuk, M. Pilkington and G. I. Nikonov, *Angew. Chem., Int. Ed.*, 2019, **58**, 18102.
- 12 A. Kempter, C. Gemel and R. A. Fischer, *Inorg. Chem.*, 2008, **47**, 7279.
- 13 M. S. Hill, P. B. Hitchcock and R. Pongtavornpinyo, *Inorg. Chem.*, 2007, **46**, 3783.
- 14 G. Tan, T. Szilvási, Sh. Inoue, B. Blom and M. Driess, *J. Am. Chem. Soc.*, 2014, **136**, 9732.
- 15 T. Chu, Y. Boyko, I. Korobkov and G. I. Nikonov, *Organometallics*, 2015, **34**, 5363.
- 16 C. Bakewell, M. Garçon, R. Y. Kong, L. O’Hare, A. J. P. White and M. R. Crimmin, *Inorg. Chem.*, 2020, **59**, 4608.
- 17 K. Nagata, T. Murosaki, T. Agou, T. Sasamori, T. Matsuo and N. Tokitoh, *Angew. Chem., Int. Ed.*, 2016, **55**, 12877.
- 18 C. Weetman, P. Bag, T. Szilvási, C. Jandl and S. Inoue, *Angew. Chem., Int. Ed.*, 2019, **58**, 10961.
- 19 C. Weetman, A. Porzelt, P. Bag, F. Hanusch and S. Inoue, *Chem. Sci.*, 2020, **11**, 4817.
- 20 T. S. Koptseva, V. G. Sokolov, S. Yu. Ketkov, E. A. Rychagova, A. V. Cherkasov, A. A. Skatova and I. L. Fedushkin, *Chem. – Eur. J.*, 2021, **27**, 5745.
- 21 V. G. Sokolov, T. S. Koptseva, R. V. Romyantsev, X.-J. Yang, Y. Zhao and I. L. Fedushkin, *Organometallics*, 2020, **39**, 66.
- 22 W. Chen, L. Liu, Y. Zhao, Y. Xue, W. Xu, N. Li, B. Wu and X.-J. Yang, *Chem. Commun.*, 2021, **57**, 6268.
- 23 I. L. Fedushkin, V. A. Dodonov, A. A. Skatova, V. G. Sokolov, A. V. Piskunov and G. K. Fukin, *Chem. – Eur. J.*, 2018, **24**, 1877.
- 24 M. V. Moskalev, A. A. Skatova, V. A. Chudakova, N. M. Khvoynova, N. L. Bazyakina, A. G. Morozov, O. V. Kazarina, A. V. Cherkasov, G. A. Abakumov and I. L. Fedushkin, *Russ. Chem. Bull.*, 2015, **64**, 2830.
- 25 O. V. Kazarina, M. V. Moskalev and I. L. Fedushkin, *Russ. Chem. Bull.*, 2015, **64**, 32.
- 26 V. G. Sokolov, T. S. Koptseva, M. V. Moskalev, A. V. Piskunov, M. A. Samsonov and I. L. Fedushkin, *Russ. Chem. Bull.*, 2017, **66**, 1569.
- 27 T. S. Koptseva, V. G. Sokolov, E. V. Baranov and I. L. Fedushkin, *Russ. J. Coord. Chem.*, 2020, **46**, 379 (*Koord. Khim.*, 2020, **46**, 333).
- 28 V. G. Sokolov, T. S. Koptseva, M. V. Moskalev, N. L. Bazyakina, A. V. Piskunov, A. V. Cherkasov and I. L. Fedushkin, *Inorg. Chem.*, 2017, **56**, 13401.
- 29 N. J. Hardman and P. P. Power, *Inorg. Chem.*, 2001, **40**, 2474.
- 30 I. L. Fedushkin, A. N. Lukoyanov, S. Y. Ketkov, M. Hummert and H. Schumann, *Chem. – Eur. J.*, 2007, **13**, 7050.
- 31 T. S. Koptseva, N. L. Bazyakina, R. V. Romyantsev and I. L. Fedushkin, *Mendeleev Commun.*, 2022, **32**, 780.
- 32 APEX3, Version 2016.9-0, Bruker, Madison, WI, 2016.
- 33 *CrysAlisPro 1.171.38.46, Data Collection, Reduction and Correction Program*, Rigaku Oxford Diffraction, 2015.

- 34 SAINT, *Data Reduction and Correction Program, Version 8.37A*, Bruker, Madison, WI, 2012.
- 35 L. Krause, R. Herbst-Irmer, G. M. Sheldrick and D. Stalke, *J. Appl. Crystallogr.*, 2015, **48**, 3.
- 36 G. M. Sheldrick, *SADABS, Version 2016/2, Bruker/Siemens Area Detector Absorption Correction Program*, Bruker, Madison, WI, 2016.
- 37 SCALE3 ABSPACK: *Empirical Absorption Correction, CrysAlisPro 1.171.38.46 - Software Package*, Rigaku Oxford Diffraction, 2015.
- 38 G. M. Sheldrick, *Acta Crystallogr.*, 2015, **A71**, 3.
- 39 G. M. Sheldrick, *Acta Crystallogr.*, 2015, **C71**, 3.
- 40 G. M. Sheldrick, *SHELXTL, Version 6.14, Structure Determination Software Suite*, Bruker, Madison WI, 2003.

Received: 12th October 2022; Com. 22/7022